Li *et al. Alzheimer's Research & Therapy* (2024) 16:211
https://doi.org/10.1186/s13195-024-01575-9

Alzheimer's
Research & Therapy

RESEARCH

Open Access

Brain Iron in signature regions relating to cognitive aging in older adults: the Taizhou Imaging Study

Rui Li[1†], Yi-Ren Fan[1†], Ying-Zhe Wang[1†], He-Yang Lu[1], Pei-Xi Li[1], Qiang Dong[1], Yan-Feng Jiang[2,3], Xing-Dong Chen[2,3*] and Mei Cui[1*]

Abstract

Background Recent magnetic resonance imaging (MRI) studies have established that brain iron accumulation might accelerate cognitive decline in Alzheimer's disease (AD) patients. Both normal aging and AD are associated with cerebral atrophy in specific regions. However, no studies have investigated aging- and AD-selective iron deposition-related cognitive changes during normal aging. Here, we applied quantitative susceptibility mapping (QSM) to detect iron levels in cortical signature regions and assessed the relationships among iron, atrophy, and cognitive changes in older adults.

Methods In this Taizhou Imaging Study, 770 older adults (mean age 62.0 ± 4.93 years, 57.5% women) underwent brain MRI to measure brain iron and atrophy, of whom 219 underwent neuropsychological tests nearly every 12 months for up to a mean follow-up of 2.68 years. Global cognition was assessed using the Mini-Mental State Examination (MMSE) and Montreal Cognitive Assessment (MoCA). Domain-specific cognitive scores were obtained from MoCA subscore components. Regional analyses were performed for cortical regions and 2 signature regions where atrophy affected by aging and AD only: Aging (AG) -specific and AD signature meta-ROIs. The QSM and cortical morphometry means of the above ROIs were also computed.

Results Significant associations were found between QSM levels and cognitive scores. In particular, after adjusting for cortical thickness of regions of interest (ROIs), participants in the upper tertile of the cortical and AG-specific signature QSM exhibited worse ZMMSE than did those in the lower tertile [β = -0.104, p = 0.026; β = -0.118, p = 0.021, respectively]. Longitudinal analysis suggested that QSM values in all ROIs might predict decline in ZMoCA and key domains such as attention and visuospatial function (all $p < 0.05$). Furthermore, iron levels were negatively correlated with classic MRI markers of cortical atrophy (cortical thickness, gray matter volume, and local gyrification index) in total, AG-specific signature and AD signature regions (all $p < 0.05$).

Conclusion AG- and AD-selective iron deposition was associated with atrophy and cognitive decline in elderly people, highlighting its potential as a neuroimaging marker for cognitive aging.

Keywords Aging-specific signature, AD signature, Iron, Atrophy, Cortical thickness, Cognition

†Rui Li, Yi-Ren Fan and Ying-Zhe Wang contributed equally to this work.

*Correspondence:
Xing-Dong Chen
xingdongchen@fudan.edu.cn
Mei Cui
cuimei@fudan.edu.cn
Full list of author information is available at the end of the article

Introduction

Cognitive aging, an inevitable, natural process of lifespan, is characterized by a progressive decline in cognitive functions, including processing speed, reasoning, and memory, among elderly individuals [1]. The rate of cognitive aging varies significantly among individuals, with those experiencing accelerated cognitive decline being at a greater risk of developing dementia [2]. In the pursuit of understanding cognitive aging, magnetic resonance imaging (MRI) has been instrumental in identifying macroscopic structural changes such as brain atrophy [3]. These changes have been extensively studied as markers of cognitive decline within community-dwelling elderly populations. However, brain atrophy represents a relatively late-stage manifestation of the cognitive decline process, prompting researchers to seek earlier and more sensitive markers.

Iron, a critical element involved in numerous biochemical processes within the brain, has emerged as a potential early biomarker for cognitive decline due to its association with neurodegenerative processes and brain aging [4, 5]. Dysregulation of cerebral iron has been implicated in the pathophysiology of several neurodegenerative diseases, suggesting that changes in iron levels may precede brain atrophy [6, 7], thus providing a window for earlier detection of cognitive decline.

Quantitative susceptibility mapping (QSM) has emerged as a reliable neuroimaging technique that facilitates noninvasive quantification of brain iron levels [8, 9]. Mounting evidence from this technique underscores its importance in deciphering the clinical progression of Alzheimer's disease (AD) and other neurodegenerative diseases [4, 5, 10]. Specifically, iron might accumulate in combination with amyloid-beta (A β), which has been shown to exacerbate cognitive deterioration [11]. Recent findings by Spotorno et al. suggest a potential relationship between iron deposition and tau aggregation, which affects brain structures [12].

Despite the promising insights provided by QSM in neurodegenerative diseases, there remains a gap in its application toward understanding cognitive aging in community-dwelling populations. Here, we conducted the QSM to investigate the potential relationship between iron deposition and cognitive aging in the Taizhou Imaging Study (TIS), a community-based prospective cohort study. First, our analysis focused on regions of interest (ROIs) to explore the association between QSM and cross-sectional and longitudinal cognition. We hypothesized that elevated local cerebral iron in cortical signature regions would be negatively related to cognitive performance. Subsequently, we conducted voxel-based QSM and morphometry analyses to compare the distribution of iron and atrophy across the whole brain among older adults with varying cognitive conditions. This study aimed to evaluate QSM as a potential imaging biomarker for the early detection of cognitive decline.

Materials and methods

Participants

The Taizhou Longitudinal Study (TZL) is an ongoing community-based prospective cohort study focused on multiple chronic diseases in rural older adults. As an ancillary study of the TZL, the TIS included four villages (Hutou, Lubao, Caixiang, and Baima) with the highest response rates, thus residents were designed to participate in the TIS, as previously described [13].

Participants from the TIS group were enrolled at baseline upon meeting the following criteria: (1) aged 45–75 years; (2) resided in Taizhou for more than 10 years; (3) had no cerebrovascular diseases, intracranial tumors, Parkinson's disease (PD), other synucleinopathies, other neurological diseases (including immune, metabolic, toxic, and infectious etiologies), or psychiatric illnesses; and (4) had complete physical, cognitive and imaging examinations. Written informed consent was obtained from all involved participants. The TIS study received ethical approval from the ethics committees of the School of Life Sciences, Fudan University, and the Fudan University Taizhou Institute of Health Sciences.

Cognitive assessments

Global cognitive function was assessed using the Mini-Mental State Examination (MMSE) and the Montreal Cognitive Assessment (MoCA). The MoCA was further subdivided into five cognitive domain scores, namely, memory (delayed recall, orientation, digit span forward), language (animal picture naming, sentence repetition), attention (serial 7 s, digit vigilance), executive function (digit span backward, trail-making test, word similarities, category fluency) and visuospatial function (cube draw, clock draw), using a method published previously [14]. Participants were categorized into three groups according to the MMSE and MoCA cutoff values [15, 16]: (1) normal cognitive function; (2) mild cognitive dysfunction; and (3) severe cognitive dysfunction.

Additionally, a comprehensive neuropsychological battery assessing the cognitive domains was executed [13]: (1) Memory: the Chinese version of the Modified Fuld Object Memory Evaluation or Auditory verbal learning test (Huashan version, AVLT-H); (2) Attention: Conflicting Instructions Task (CIT); (3) Execution: Trail Making Test (TMT); (4) Language: Animal Naming Test (ANT); and (5) Visuospatial function: Clock Drawing Test (CDT). Dementia and mild cognitive impairment (MCI) were diagnosed by the consensus of neurologists with the criteria in the Diagnostic and Statistical Manual

of Mental Disorders, fifth edition (DSM-5) [17] and the criteria proposed by Petersen [18], respectively. The two categorical approaches, though differing in criteria, complement each other in their applicability. Clinical diagnosis reflects reliably cognitive status and aligns closely with clinical practice, allowing voxel-based analyses in our study, while scale-based diagnosis expands the sample size and offers a pragmatic approach suitable for community screening, providing a baseline adjustment in our analyses. All cognitive scores were standardized into Z scores.

MRI acquisition and preprocessing

MRI data were obtained using 3.0 T MR scanners at two sites, including 3D T1-weighted magnetization-prepared rapid gradient echo (MPRAGE), fluid-attenuated inversion recovery (FLAIR), and multiecho gradient-recalled echo (GRE) sequences with the following acquisition parameters, respectively: slice thickness = 1.0 mm, TR = 2300 ms, TE = 2.98/2.26 ms, FA = 8/9°; slice thickness = 2.0/3.0 mm, TR = 8000/9110 ms, TE = 94/96 ms, FA = 150°; slice thickness = 1.5 mm, TR = 28 ms, TE 1 = 20 ms, TE 2 = 15 ms, ΔTE = 5 ms, FA = 15°. All MR images were reviewed by trained neuroradiologists. The detailed MRI sequences at each site are described in Supplemental Table 1.

Integration of T1-weighted structural and FLAIR images was applied to improve pial surfaces in the FreeSurfer v7.2.0 pipeline (http://surfer.nmr.mgh.harvard.edu). Segmentations were visually inspected for both internal and external surfaces following the ENIGMA Cortical Quality Control Protocol 2.0 [19].

QSM reconstruction

QSM reconstruction was conducted using the combined pipeline in Sepia v0.8.1.1 (https://github.com/kschan0214/sepia) [20]. In summary, the phase images were spatially unwrapped with a Laplacian-based technique [21]. Binary masks, which are necessary for distinguishing local from background fields, were created via the 'antsBrainExtraction.sh' approach in ANTs (version 2.3.5, https://github.com/ANTsX/ANTs) based on the magnitude images. The variable-kernels sophisticated harmonic artifact reduction for phase data (V-SHARP) algorithm was employed for background field removal, with a radius of a spherical mean value (SMV) kernel of 12 mm [22]. During this processing step, the masks were eroded by 2 voxels from the edge of the brain. Finally, susceptibility maps were reconstructed using the improved sparse linear equations and least squares (iLSQR) algorithm [23]. To mitigate assumptions about areas being spared in aging and minimize potential errors caused by reference selections, QSM values were not referenced, as suggested by previous studies [24, 25].

Cortical signature measurements

Bias-corrected magnitude gradient echo images were affinely coregistered to their corresponding bias-corrected MPRAGE volume. Subsequently, the QSM images were linearly registered to the MPRAGE volumes. Bias correction was performed using the N4 algorithm (ANTs).

Assuming that iron concentration in regions affected by normal aging and AD is relevant to cognitive aging, we computed three cortical signature QSMs in the native space (Supplemental Table 2; Supplemental Fig. 1): AD signature ROI based on work by Jack et al. [26] and Aging (AG)-specific signature ROI proposed by Dickerson and colleagues [27]. The AD signature meta-ROI were defined as the entorhinal, fusiform, inferior temporal, and middle temporal cortex regions. The AG-specific signature meta-ROI represents a map of specific brain regions involved in cortical atrophy due to aging only, consisting of the inferior and dorsomedial frontal, precentral, fusiform, lateral occipital, cuneus, pericalcarine, and caudal insula cortex regions.

MRI-derived markers for neurodegeneration [cortical thickness, gray matter (GM) volume, local gyrification index and surface area] were also computed for these cortical signature regions. The estimated total intracranial volume (eTIV) was used to normalize the total brain and GM volume without ventricles to determine global and GM atrophy, respectively. All segments were inferred from anatomical MPRAGE images in the FreeSurfer v7.2.0 framework. The values of the ROIs were averaged across hemispheres for QSM and structural MRI analyses.

Voxel-based QSM analysis

The MPRAGE images were nonlinearly registered to the MNI space (Montreal Neurological Institute, McGill University, Canada) using the SyN algorithm (ANTs). QSM data were spatially standardized to the MNI space by concatenating the warp of the aforementioned transformations and applying third-order b-spline interpolation. Absolute QSM maps were used for whole-brain analysis to prevent convolution-driven cancellations of spatially adjacent positive/negative susceptibilities. To attenuate the spurious impact of brain boundary effects, a 3D Gaussian kernel with a standard deviation of 3 mm was applied for smoothing, followed by a previously proposed smoothing-compensation strategy [25, 28]. The QSM maps were confined to GM regions using probabilistic tissue segments obtained from MPRAGE data using SPM12 tissue segmentation (http://www.fil.ion.ucl.ac.uk/spm/software/spm12). Finally, whole-brain (dementia

vs. MCI vs. CN) analysis was carried out using nonparametric permutation testing (10,000 permutations) with threshold-free cluster enhancement (TFCE) implemented in FSL randomize v2.9 (with '-T' settings, http://fsl.fmrib.ox.ac.uk/fsl/fslwiki/Randomize). The statistical model included age and sex as nuisance covariates. Significant clusters were reported at FWE-corrected P values < 0.05.

Voxel-based gray matter volume analysis

All the MPRAGE images were extracted from the brain via ANT and GM segmentation in SPM12. To perform a simultaneous analysis pipeline for voxel-based morphometry (VBM) and QSM, the subsequent procedures were performed and adhered to FSL-VBM routines. First, GM images were nonlinearly registered to the MNI152 template, concatenated and averaged to create a study-specific GM template. Second, all native GM images were then reregistered to this study-specific template using nonlinear registration. Third, each registered GM image was multiplied by the Jacobian of the warp field for modulation to account for volume changes during registration. Fourth, all the modulated registered GM images were then smoothed using a Gaussian kernel with a standard deviation of 3 mm. Finally, we conducted a random analysis and displayed TFCE-based thresholding results with the same permutation testing settings as mentioned above.

Statistical analysis

All the statistical analyses were performed using R (version 4.3.1) provided by the R Core Team (2023) (R: a language and environment for statistical computing; R Foundation for Statistical Computing, Vienna, Austria). Multiple linear regression models were used to explore the associations between brain iron signatures, as measured by signed ROI-QSMs (cortical and signature brain regions), and age, MRI markers, and cross-sectional cognitive performance (n = 770). Regarding baseline cognition, the ROI-QSM values were stratified into tertiles for potential threshold effects and simplified interpretations, while continuous values were analyzed in the supplement. Further, subregional analyses for signature QSMs which survived FDR correction were performed in the supplement. Linear mixed-effect models were utilized to investigate the longitudinal relationship between ROI-QSM values and cognitive function over time (n = 219). To assess the independence of these associations from local cerebral atrophy, models were rerun with additional control for local cortical thickness or volume in each ROI (Model 3). Comparisons with lobar and subcortical QSMs were detailed in the supplement. Finally, voxel-based morphometry and QSM analyses were conducted in individuals who had available baseline cognitive diagnoses (N = 458) to assess the capacity of iron spatial deposition associated with atrophy and cognitive impairment across the whole brain. The site effect was added as covariate to all statistical models to minimize potential site-related differences. A two-sided P value < 0.05 was considered indicative of a significant difference, and Benjamini–Hochberg correction was applied for multiple comparisons [29].

Results

Participant characteristics

A total of 925 participants aged 45–75 years were enrolled from 2017 to 2022. Among 925 participants, 155 individuals were excluded due to missing clinical tests, SWI scans, neurological disease, conflicting cognitive status and poor MRI quality, resulting in a final sample size of 770 individuals (Fig. 1). The vast majority of participants were cognitively intact according to MMSE, with 81.9% scoring > cutoff. Among them, 458 participants completed the full neuropsychological battery and were diagnosed with cognitively normal (CN; N = 290), MCI (N = 140) and dementia (N = 28). Cognitive follow-up assessments were conducted at two distinct intervals, with 770 participants involved. During the first follow-up period (2019–2020), 416 individuals were not included because they had not reached the follow-up time point, and 293 participants completed the assessment. This number further decreased to 219 participants in the subsequent follow-up period (2020–2021). The retention rates were 82.8% (293/354) and 85.5% (219/256), respectively. The flow chart of the selection process is shown in Fig. 1. The demographic information and neuropsychological data of the 770 participants are summarized in Table 1. We also compared the characteristics between individuals who were followed up and those who were not among the two groups (Supplemental Table 3).

Relationship between iron signatures and cross-sectional cognition

The study examined the correlation between age and QSM values across various brain regions. As shown in Supplemental Fig. 2, the QSM values in the cortical (β = 0.098, p = 0.026), AG-specific signature (β = -0.091, p = 0.030) and AD signature (β = 0.109, p = 0.026) regions were all positively correlated with age. These findings suggest that age may be a significant risk factor for increased iron deposition.

The relationship between iron deposition in different brain regions and baseline global cognitive scores was then examined. As shown in Table 2, participants in the tertile 3 of the cortical QSM presented significantly poorer ZMMSE (β = -0.100, p = 0.026) than did those in

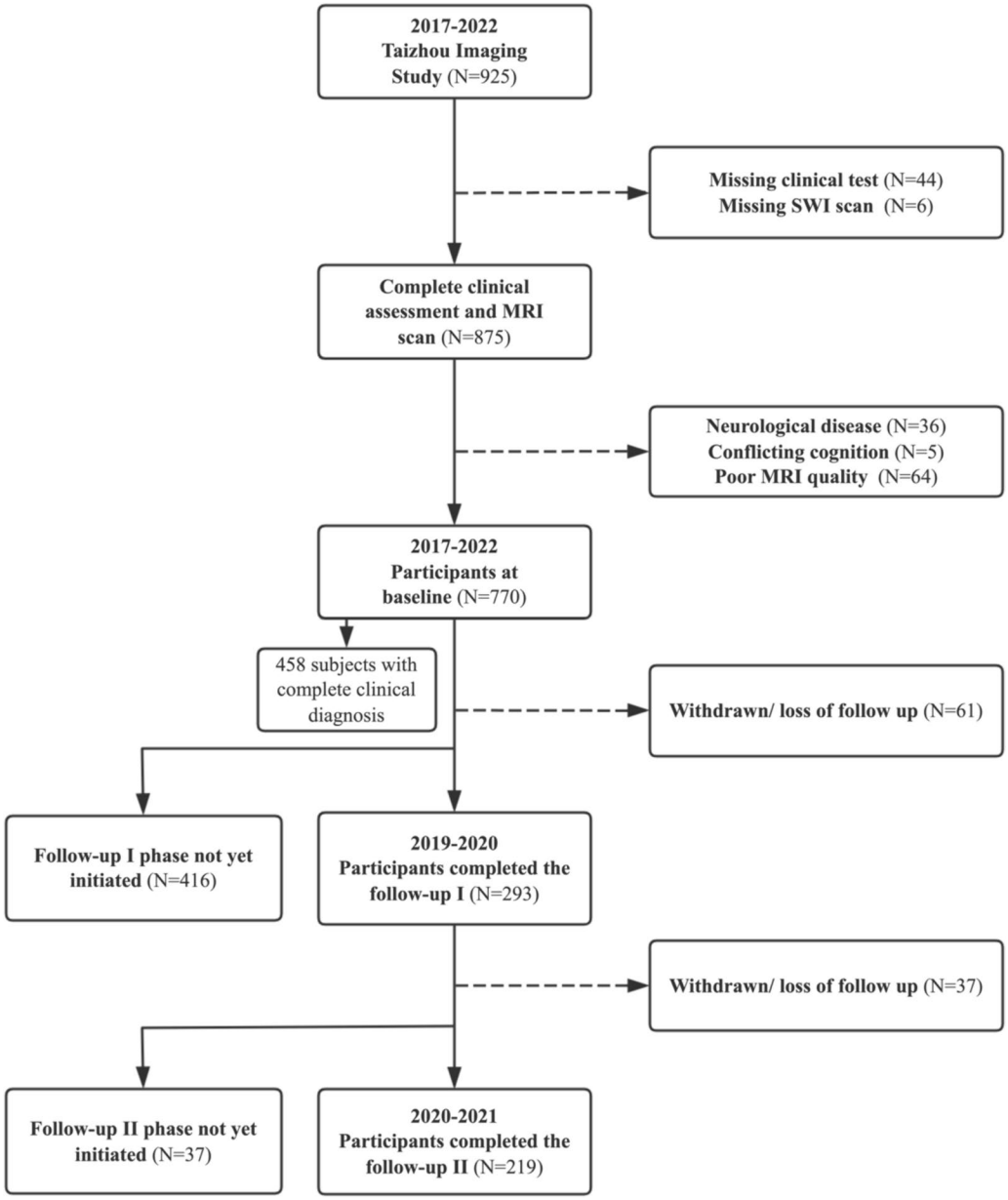

Fig. 1 Flowchart of this study

the tertile 1 after adjusting for sex, age, education, site, eTIV, cognitive status, smoking, drinking, and medical history (Model 2), as well as in the AG-specific signature QSM (β = -0.110, p=0.026). This association persisted even after accounting for cortical thickness (interpreted as local atrophy) of the ROI (Model 3; β = -0.104, p=0.026; β = -0.118, p=0.021, respectively). Concordant with the findings of ROI-QSMs in tertiles, continuous QSM values in the cortical and AG-specific signature regions returned significant correlations with ZMMSE (Supplemental Table 4; Model 1; β = -0.036, p=0.050; β = -0.035, p=0.050, respectively). Specifically, subregional analyses revealed that only the tertile 3 of dorsomedial frontal QSM signal was negatively correlates with ZMMSE compared to tertile 1 (Supplemental Table 5; Model 3; β = -0.119, p=0.036). However, similar negative correlations between brain iron and global cognition were not observed in the AD signature regions. In summary, higher QSM values were linked to lower ZMMSE, particularly in aging-selective and cortical regions. Nevertheless, no significant correlations were found between QSM in any of the selected ROIs and the ZMoCA.

Table 1 Baseline demographical, clinical and MRI characteristics of participants

	Baseline (*n* = 770)
Demographics	
Age, y	62.0 ± 4.93
Male	327 (42.5)
Education, y	5.35 ± 3.80
Cognition	
Baseline MMSE, score	26.0 (22.0, 28.0)
Baseline MoCA, score	18.0 (13.0, 22.0)
Follow-up MMSE[a], score	25.0 (22.0, 27.0)
Follow-up MoCA[a], score	17.0 (13.0, 21.0)
Follow-up time[a], year	2.68 ± 0.39
Neuroimaging	
Cortical QSM	0.74 ± 0.78
AG-specific signature QSM	2.02 ± 0.93
AD signature QSM	1.26 ± 1.80
Global atrophy	0.70 ± 0.04
Gray matter atrophy	0.38 ± 0.02

Data are mean ± SD, n (%), or median (interquartile range)

Demographic information and clinical characteristics were compared using 2, Student t-test and Mann-Whitney U-test

Abbreviations: *AD* Alzheimer's disease, *AG* Aging, *MMSE* Mini-Mental State Examination, *MoCA* Montreal Cognitive Assessment, *QSM* Quantitative susceptibility mapping

[a] Data were summarized in subjects who completed follow-up phase I and II (*n* = 219)

Relationship between iron signatures and local cortical atrophy

The study evaluated the associations between QSM values in different brain regions and regional brain atrophy. As shown in Fig. 2 and Supplemental Table 6, after adjusting for sex, age, education, site, smoking, drinking, history of disease, and cognition, the QSM values in the cortical, AG-specific signature and AD signature regions remained significantly negatively correlated with cortical thickness (Model 3; $p < 0.005$). Similar significant negative correlations were also observed for other MRI-classical indicators reflecting neurodegeneration, such as GM volume and local gyrification index (Fig. 2). However, there were no significant correlations between QSM in any of the selected ROIs and surface area.

Relationship between iron signatures and longitudinal cognition

QSM values in all selected ROIs were associated with cognitive decline as assessed by the MoCA (Table 3). In participants who completed baseline assessments and two cognitive follow-ups ($n = 219$), the annual decrease in MoCA scores was negatively correlated with iron deposition in the cortical (β = -0.440, $p = 0.009$), AG-specific signature (β = -0.527, $p = 0.002$) and AD signature regions (β = -0.365, $p = 0.029$) after adjusting for sex, age, education, eTIV, smoking, drinking, and history of disease (Model 2). These associations with longitudinal changes in the MoCA scores remained significant independent of local atrophy after additionally adjusting for the cortical thickness of each ROI (Model 3; $p < 0.05$). Considering the differences in scale sensitivity, we did not observe any relationship between QSM in any of the selected ROIs and longitudinal changes in MMSE scores.

Analyses of domain-specific cognitive scores (from MoCA components) also confirmed such negative associations in all ROI-QSMs. Decreased attention was predicted by brain iron levels in the cortical (Model 3; β = -0.380, $p = 0.024$), AG-specific signature (β = -0.356, $p = 0.033$) and AD signature (β = -0.347, $p = 0.039$) regions, independent of atrophy, as depicted in Fig. 3. Additionally, a negative association was also observed between the rate of change in visuospatial function and cortical as well as all signature QSMs (Model 3; β = -0.464, $p = 0.006$; β = -0.335, $p = 0.045$; β = -0.491, $p = 0.003$, respectively). Regarding executive function, QSM in the AD signature region was predictive of a steeper decline (Model 3; β = -0.411, $p = 0.014$), while QSM in the AG-specific signature region predicted language decline (Model 3; β = -0.418, $p = 0.012$). However, no significant correlations were found between QSM values in any of the selected ROIs and episodic memory (Supplemental Table 7).

Notably, analysis including lobar and subcortical ROIs showed the AD signature QSM no longer correlates with annual decline in ZMoCA (Supplemental Table 9). Still, QSM in the cortical and AG-specific signature regions could predict longitudinal decline in ZMoCA (Model 3; $p < 0.05$). Similarly, the frontal lobe QSM exhibited a significant negative correlation with ZMoCA deterioration (Model 3; β = -0.544, $p = 0.013$). Unfortunately, this negative correlation between iron load and ZMMSE did not persist in the frontal lobe after additionally adjusting for local cortical thickness, nor in the amygdala and caudate after accounting for local volume (Model 3). Non-significant associations with cognitive changes were observed in other traditional lobar and subcortical QSMs.

Iron metabolism patterns across cognitive diagnoses: voxel-based QSM analysis

Voxel-based comparisons of QSM values were conducted among the CN, MCI, and dementia groups (CN = 290; MCI = 140; dementia = 28). Within the dementia group, elevated QSM values were observed in five distinct clusters compared to those in the CN group (Fig. 4; Supplemental Table 8). Pronounced abnormalities were

Table 2 Association between localized QSM and baseline global cognition

		ZMMSE		ZMoCA	
		β(95% CI)	*P*	*β*(95% CI)	*P*
Cortical QSM					
T2 vs. T1	Model 1	-0.070 (-0.150, 0.010)	0.298	-0.092 (-0.177, -0.008)	0.126
	Model 2	-0.068 (-0.150, 0.013)	0.298	-0.096 (-0.181, -0.010)	0.126
	Model 3	-0.069 (-0.152, 0.013)	0.298	-0.090 (-0.177, -0.003)	0.126
T3 vs. T1	Model 1	-0.107 (-0.189, -0.026)	**0.022**	-0.022 (-0.108, 0.064)	0.986
	Model 2	-0.100 (-0.183, -0.018)	**0.026**	-0.013 (-0.100, 0.074)	0.986
	Model 3	-0.104 (-0.189, -0.018)	**0.026**	-0.002 (-0.092, 0.088)	0.986
AG-specific signature QSM					
T2 vs. T1	Model 1	-0.027 (-0.106, 0.052)	0.503	-0.070 (-0.153, 0.014)	0.203
	Model 2	-0.029 (-0.109, 0.050)	0.503	-0.068 (-0.153, 0.016)	0.203
	Model 3	-0.032 (-0.112, 0.048)	0.503	-0.064 (-0.148, 0.021)	0.211
T3 vs. T1	Model 1	-0.119 (-0.198, -0.040)	**0.021**	-0.011 (-0.095, 0.073)	0.986
	Model 2	-0.110 (-0.190, -0.030)	**0.021**	-0.001 (-0.085, 0.084)	0.986
	Model 3	-0.118 (-0.201, -0.036)	**0.021**	0.013 (-0.075, 0.100)	0.986
AD signature QSM					
T2 vs. T1	Model 1	-0.047 (-0.127, 0.032)	0.503	-0.038 (-0.122, 0.047)	0.491
	Model 2	-0.037 (-0.118, 0.044)	0.503	-0.029 (-0.114, 0.057)	0.523
	Model 3	-0.036 (-0.117, 0.045)	0.503	-0.028 (-0.114, 0.058)	0.523
T3 vs. T1	Model 1	-0.036 (-0.118, 0.046)	0.507	-0.007 (-0.093, 0.080)	0.986
	Model 2	-0.027 (-0.109, 0.056)	0.570	-0.001 (-0.088, 0.087)	0.986
	Model 3	-0.024 (-0.107, 0.059)	0.570	0.001 (-0.087, 0.089)	0.986

Standardized Beta coefficient values represent a one unit change in global cognition z-score with a one PPB change in QSM

Model 1 was adjusted for sex, age, years of education, site, eTIV, and cognitive status

Model 2 was additionally adjusted smoking, drinking, hypertension, diabetes, and hyperlipidemia

Model 3 was additionally adjusted cortical thickness of each ROI

Abbreviations: *AD* Alzheimer's disease, *AG* Aging, *MMSE* Mini-Mental State Examination, *MoCA* Montreal Cognitive Assessment, *QSM* Quantitative susceptibility mapping, *T1* 1st tertile, *T2* 2nd tertile, *T3* 3rd tertile

Benjamini-Hochberg FDR corrected $P < 0.05$ are shown bold

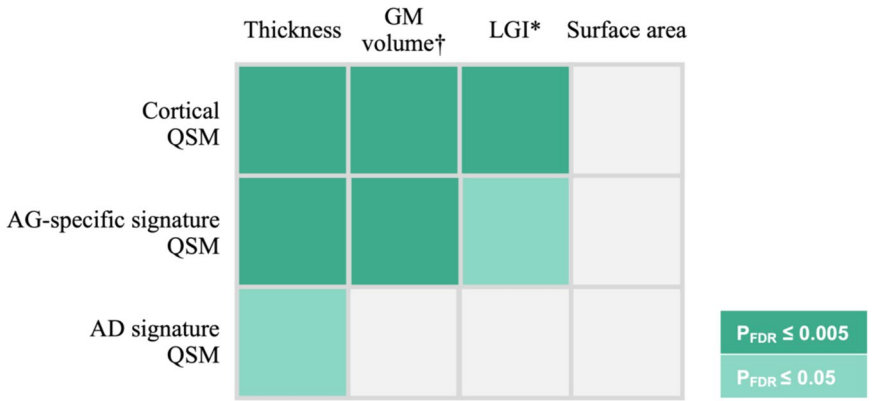

Fig. 2 Association between MRI markers of local cortical atrophy and QSM in signature regions. †Gray matter volume was normalized by eTIV. *Data were missing in 5 of 770, 0.6%. Abbreviations: AD = Alzheimer's disease; AG = Aging; GM = Gray matter; LGI = Local gyrification index; QSM = quantitative susceptibility mapping

Table 3 Association between localized QSM and longitudinal global cognition

	change in ZMMSE		change in ZMoCA	
	β(95% CI)	*P*	*β*(95% CI)	*P*
Cortical QSM				
Model 1	-0.162 (-0.488, 0.164)	0.329	-0.433 (-0.758, -0.109)	**0.009**
Model 2	-0.165 (-0.495, 0.165)	0.326	-0.440 (-0.769, -0.112)	**0.009**
Model 3	-0.164 (-0.495, 0.166)	0.329	-0.441 (-0.770, -0.112)	**0.009**
AG-specific signature QSM				
Model 1	-0.220 (-0.544, 0.104)	0.184	-0.526 (-0.847, -0.204)	**0.001**
Model 2	-0.222 (-0.549, 0.105)	0.182	-0.527 (-0.851, -0.202)	**0.002**
Model 3	-0.221 (-0.548, 0.106)	0.185	-0.526 (-0.850, -0.201)	**0.002**
AD signature QSM				
Model 1	-0.087 (-0.411, 0.236)	0.595	-0.354 (-0.677, -0.032)	**0.031**
Model 2	-0.090 (-0.419, 0.239)	0.592	-0.365 (-0.693, -0.037)	**0.029**
Model 3	-0.092 (-0.421, 0.238)	0.585	-0.364 (-0.692, -0.035)	**0.030**

Standardized Beta coefficient values represent a one unit change in global cognition z-score per 1 years with a one PPB change in QSM

Model 1 was adjusted for sex, age, years of education and eTIV

Model 2 was additionally adjusted smoking, drinking, hypertension, diabetes, and hyperlipidemia

Model 3 was additionally adjusted cortical thickness of each ROI

Abbreviations: AD = Alzheimer's disease; AG = Aging; MMSE = Mini-Mental State Examination; MoCA = Montreal Cognitive Assessment; QSM = quantitative susceptibility mapping

Benjamini-Hochberg FDR corrected $P < 0.05$ are shown bold

identified in the left frontal pole/middle frontal gyrus/superior frontal gyrus ($p = 0.018$); left paracingulate gyrus/superior frontal gyrus/frontal pole ($p = 0.040$); left paracingulate gyrus/medial frontal cortex/cingulate gyrus ($p = 0.041$); left caudate/accumbens/putamen/subcallosal cortex ($p = 0.036$); and left frontal pole ($p = 0.049$). In addition, the dementia group exhibited greater QSM signal in the left middle frontal gyrus/superior frontal gyrus/frontal pole than did the MCI group ($p = 0.031$). There were no significant regions where the MCI group had higher QSM values than did the HC group. Furthermore, VBM analysis revealed no discernible differences in atrophy across the aforementioned groups at a whole-brain FDR-corrected $p < 0.05$.

Discussion

In this study, our focus was on iron deposition in regions selectively associated with aging and AD, aiming to evaluate its correlation with baseline cognition and assess its potential value in predicting future cognitive decline processes. Here, for the first time, we present evidence linking increased iron levels in signature brain regions to exacerbated cognitive decline and structural brain alterations in a community-based cohort. The whole-brain approach allows for the mapping of iron distribution, revealing increased iron load in dementia patients across the frontal, paracingulate, and cingulate cortex, as well as in deep gray matter structures such as the caudate, accumbens, and putamen. In agreement with previous studies indicating iron-related cognitive dysfunction [30–32], our findings support the potential of brain iron overload as a neuroimaging marker for the early assessment of cognitive decline in elderly individuals within a community setting.

The pathological deposition of cerebral iron significantly contributes to the cascade of neurodegenerative processes. Excessive iron accelerates the production of reactive oxygen species (ROS), leading to oxidative stress that damages neuronal lipids, proteins, and DNA [33]. Furthermore, the interaction of iron with activated microglia promotes neuroinflammatory responses, exacerbating neuronal damage [34]. Interestingly, our study found that cross-sectional associations between some ROI-QSM values and ZMMSE were stronger compared to ZMoCA. This suggests MMSE may better capture certain neurodegenerative changes reflected in QSM. Conversely, longitudinal outcomes reveal that MoCA, with its comprehensive assessment of multiple cognitive domains, may be more sensitive to subtle and early changes in cognition over time [35]. Longitudinal studies further emphasize the dynamic relationship between QSM changes and cognitive scores, where MoCA may reveal changes not captured by MMSE due to its broader scope.

The dorsomedial frontal region is integral to executive function, decision-making, and cognitive control, domains assessed by the MMSE. Research indicates that age-related atrophy in this region correlates with declines in these cognitive areas [36], explaining the significant ZMMSE differences observed between the upper and bottom QSM tertiles in our study. This finding highlights the importance of the dorsomedial frontal region within the AG-specific signature ROI, as it may capture critical aging-related iron concentration affecting cognitive performance. Furthermore, we found that iron deposition in total cortical and AG-specific signature regions more accurately predicts decline in ZMoCA compared to traditional lobar and subcortical ROIs. By focusing on the signature ROIs, our study provides a more precise analysis of the effects of normal aging on brain structures and cognition, and underscores a potential and surrogate advantage of cortical signature QSMs in detecting early cognitive decline, which is crucial for understanding the nuances of cognitive aging.

Iron deposition in the brain plays a pivotal role in the progression of neurodegenerative changes and may lead to brain atrophy through several interrelated mechanisms. Iron overload may facilitate brain atrophy through ferroptosis, a nonapoptotic cell death pathway,

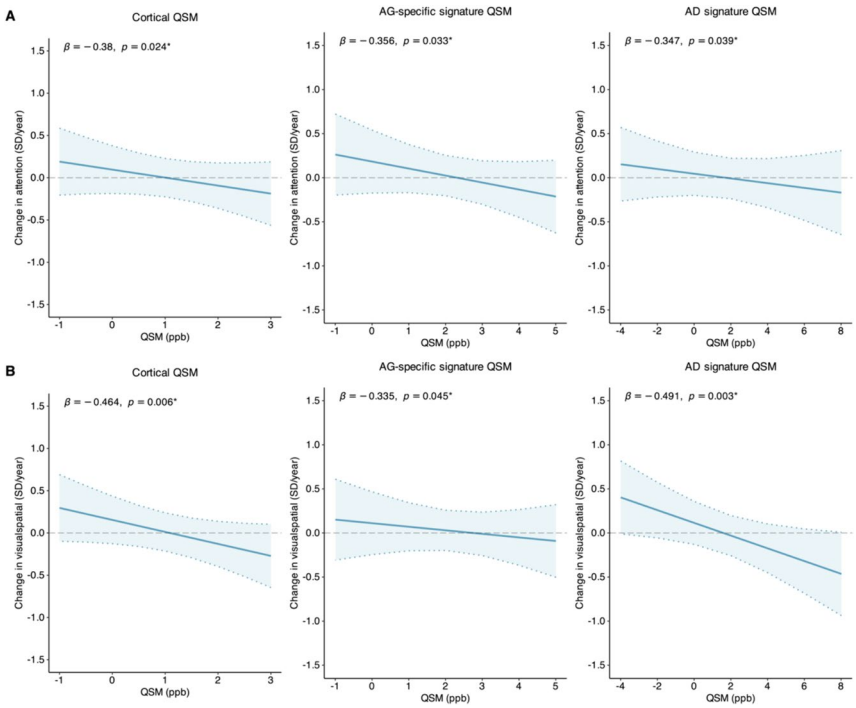

Fig. 3 Association between localized QSM and longitudinal domain-specific cognitive score changes. **A**, **B** Trajectory plots illustrate the impact of baseline QSM on the change in longitudinal attention and visuospatial function. The annual rate of domain-specific cognitive decline was calculated for each individual and plotted against the baseline localized QSM values. Estimated cognitive trajectories with 95% confidence intervals (CIs) are displayed. The model is adjusted for sex, age, years of education, smoking, drinking, hypertension, diabetes, and hyperlipidemia, eTIV and cortical thickness of each ROI (Supplemental Table 7; Model 3). Abbreviations: AD = Alzheimer's disease; AG = Aging; QSM = quantitative susceptibility mapping

by catalyzing reactive oxygen species production and promoting lipid peroxidation, leading to neuronal damage and cell death [37]. Moreover, the interaction of iron with critical proteins, including tau, exacerbates their pathological aggregation, further implicating iron in the progression of AD, which facilitates neuronal damage and brain atrophy [38]. Additionally, iron-induced neuroinflammation, characterized by activated microglia and the release of proinflammatory cytokines, accelerates brain tissue loss [39]. A seven-year follow-up longitudinal study by Daugherty et al. [40] reported that increased iron levels, particularly in the putamen, predict accelerated brain shrinkage in 32 older adults. In support of this, our research revealed that iron level correlates with atrophy in signature brain regions, affecting cortical thickness, gray matter volume, and LGI. Although the causal relationship between iron deposition and brain atrophy, particularly in the context of aging and AD, remains to be fully elucidated, further investigation into the role of iron in the neurodegenerative cascade is necessary.

The sensitivity of QSM in neuroimaging studies offers promising insights into the distribution of iron levels in key brain regions, including the hippocampus, amygdala, and caudate, in AD patients [41]. Moreover, widespread increased magnetic susceptibility across the cortical ribbon, asymmetrically covering the left hemisphere cerebral cortex, caudate nucleus, putamen, and partial cerebellar cortex, as demonstrated in another study [42], points to a complex pattern of neurodegeneration uniquely captured by QSM. Specifically, subcortical iron content has been proposed as a potential biomarker for subcortical vascular MCI [43]. However, our whole-brain volumetry analysis did not align with these QSM findings, suggesting that overall, QSM may be more sensitive than conventional structural MRI in detecting abnormalities in MCI and dementia patients and could also be an indication that QSM might capture early pathological changes before volumetric losses are evident.

The phenomenon of brain iron concentration, while critical to the pathology of cognitive decline, remains only partially understood. Its development is influenced by a constellation of factors, including genetic predispositions that disrupt normal iron metabolism and regulatory mechanisms. Notably, conditions such as neurodegeneration with brain iron accumulation (NBIA) underscore the genetic component of this pathology [44]. Age-related factors also play a vital role, with evidence suggesting that the brain's ability to regulate iron

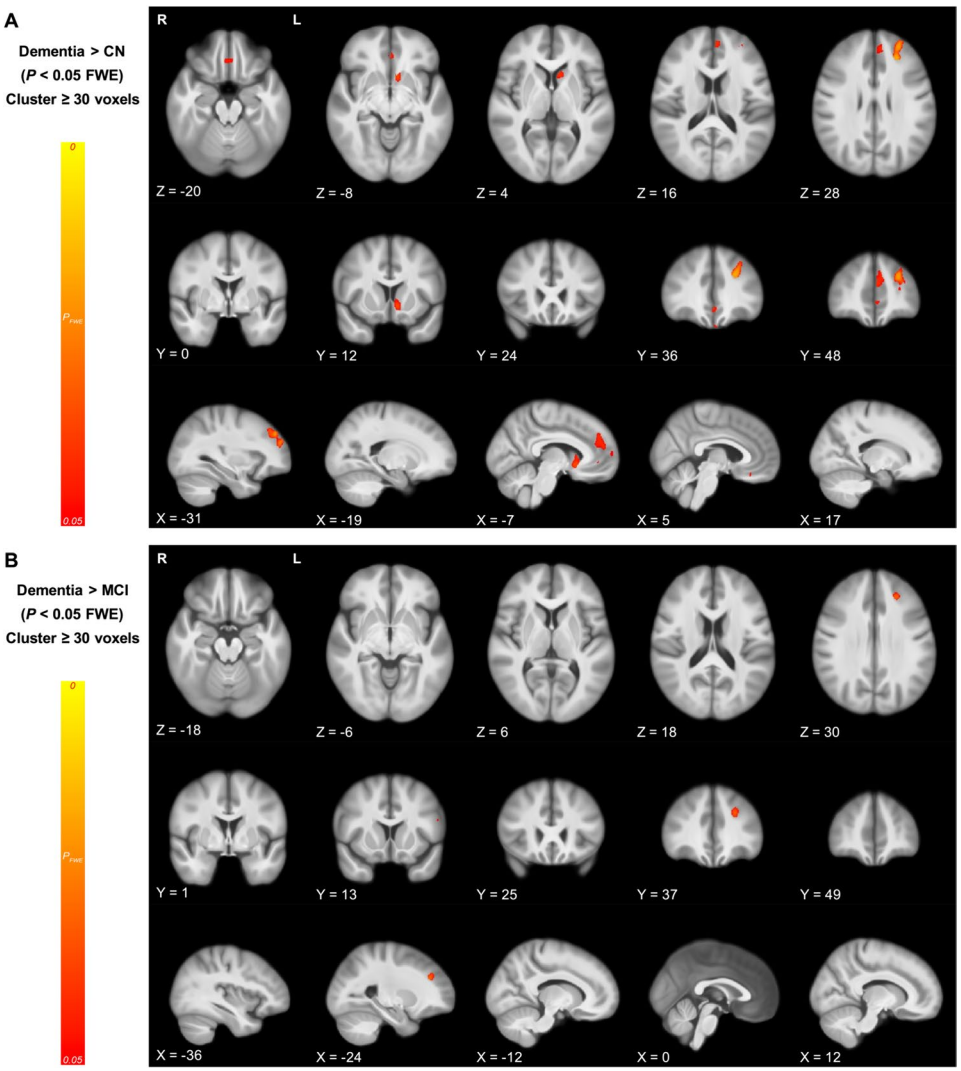

Fig. 4 Distribution of increased brain iron in dementia compared to CN and MCI. **A** Red/yellow clusters represent significantly higher QSM values in the dementia group than in the CN group. **B** absolute QSM was greater in the dementia group than in the MCI group. 458 participants with complete cognitive diagnosis were included in this analysis: CN = 290; MCI = 140; dementia = 28. The results were overlaid onto the study-wise anatomical template in the MNI (Montreal Neurological Institute template) space and displayed in radiological orientation. Abbreviations: CN = cognitively normal; FWE = family-wise error; MCI = mild cognitive impairment; QSM = quantitative susceptibility mapping

diminishes with age, leading to iron accumulation in specific regions associated with motor and cognitive functions [5]. Our investigation confirmed the age-associated concentration of iron in cortical, AG-specific signature and AD signature regions, aligning with multiple studies that have demonstrated a widespread pattern of iron load across various subcortical structures (e.g., the GP, putamen, amygdala, hippocampus, SN, and RN) and cortical regions (e.g., all lobes and the entorhinal, ITG, SMF and IOF cortices) during aging [45–47]. Furthermore, dysfunction of the blood-brain barrier (BBB) represents a crucial mechanism for abnormal iron deposition, particularly in neurodegenerative conditions such as PD [48]. Collectively, these findings highlight the multifaceted nature of brain iron deposition and its implications for neurodegenerative diseases.

The negative findings from the FAIRPARK-II trial [49], where iron chelation therapy with deferiprone led to clinical worsening in PD patients, highlighted the necessity of carefully navigating the delicate balance between the indispensable physiological role of iron and its propensity to inflict damage when present in excess. This revelation does not diminish the significance of our research but rather emphasizes the need for a sophisticated approach

to dissect the intricate interactions among iron-related neurodegenerative mechanisms. Our study specifically addresses the issue of iron load and its correlation with cognitive decline in signature brain regions, aiming to uncover biomarkers for early detection and intervention. This work holds promise for revealing novel avenues for understanding and treating neurodegeneration in aging populations.

This study is subject to several limitations. First, not all participants completed consecutive follow-ups from baseline, resulting in a relatively limited number of subjects for the longitudinal analysis. This lack of consistency increases the risk of false-negative associations. Second, due to the absence of continuous scans in the current study, we were unable to assess the dynamics of iron accumulation and its relationship with brain shrinkage and cognitive changes. Further investigations with larger longitudinal datasets are therefore warranted. Third, this study did not incorporate cerebrospinal fluid or plasma biomarker evidence of cerebral amyloid and tau pathology (e.g., Aβ42, Aβ42/40 ratio, total-tau, and p-tau), which could have provided valuable insights into iron-related mechanisms. Further research is needed to explore these potential connections. Finally, while QSM is sensitive to variations in brain iron content, it is important to note that magnetic susceptibility, as measured by QSM, may also be influenced by other metals (e.g., copper, manganese aluminum, and calcium) [50], myelin [51] and cellular packing density [52]. Variations in QSM reconstruction, spatial standardization, and other procedures may introduce biases that could impact the generalizability of our study findings. Therefore, these factors should be carefully considered when interpreting the results.

Conclusion

Overall, this study revealed that our distinctive signature QSMs were capable of identifying individuals at risk of cognitive aging in the community elderly. The spatial concentration of iron correlates with dementia, offering novel insights into the role of iron deposition in the aging population. Although iron deposition in specific brain regions has been extensively studied, the signature patterns of iron overload in age-related brain areas still warrant further investigation.

Abbreviations

AD	Alzheimer's disease
AG	Aging
Aβ	Amyloid-beta
BBB	Blood–brain barrier
eTIV	estimated total intracranial volume
FLAIR	Fluid-attenuated inversion recovery
GM	Gray matter
GRE	Gradient-recalled echo sequence
MCI	Mild cognitive impairment
MMSE	Mini-Mental State Examination
MNI	Montreal Neurological Institute
MoCA	Montreal Cognitive Assessment
MPRAGE	Magnetization-prepared rapid gradient echo
MRI	Magnetic resonance imaging
PD	Parkinson's disease
QSM	Quantitative susceptibility mapping
ROIs	Regions of interest
TIS	Taizhou Imaging Study
TZL	Taizhou Longitudinal Study
VBM	Voxel-based morphometry

Supplementary Information

The online version contains supplementary material available at https://doi.org/10.1186/s13195-024-01575-9.

Supplementary Material 1.

Acknowledgements

The authors thank the study participants and the staff of Huashan Hospital Fudan University and the Fudan University Taizhou Institute of Health Sciences for assistance in neighborhood outreach and engagement in support of participant recruitment.

Authors' contributions

R.L. and Yr.F. were responsible for the study design, statistical analysis, and writing of the original draft of the manuscript. Yz. W., Hy. L, and Px. L participated in the data collection and figure preparation. Q.D. and Yf. J reviewed and edited the manuscript. Xd.C. and M.C. engaged in the study design and study supervision. All the authors contributed to the final version of the paper.

Funding

The study was supported by the following agencies: the National Key R&D Program of China (2021YFC2500100), the Ministry of Science and Technology of China STI2030-Major Projects (2021ZD0201806), the Science and Technology Innovation 2030 Major Projects (2022ZD0211600), the Key Research and Development Plans of Jiangsu Province, China (BE2021696), and the Shanghai Municipal Science and Technology Major Project (2023SHZDZX02).

Availability of data and materials

The datasets supporting this study's findings were obtained from the TIS cohort, which is available from the corresponding author upon request to any qualified investigator subject to a data use agreement (Mei Cui, e-mail: cuimei@fudan.edu.cn).

Declarations

Ethics approval and consent to participate

The study was approved by the ethics committees of the School of Life Sciences, Fudan University, and the Fudan University Taizhou Institute of Health Sciences. The research was conducted in accordance with the Declaration of Helsinki. Written informed consent was obtained from all participants involved in the Taizhou Imaging Study.

Consent for publication

Not applicable.

Competing interests

The authors declare no competing interests.

Author details

[1]Department of Neurology, Huashan Hospital, State Key Laboratory of Medical Neurobiology and MOE Frontiers Center for Brain Science, Fudan University, No. 12 Middle Wulumuqi Road, Shanghai 200040, China. [2]State Key Laboratory of Genetic Engineering, Zhangjiang Fudan International Innovation Center, Human Phenome Institute, Fudan University, 2005 Songhu Road, Shanghai 200438, China. [3]Fudan University Taizhou Institute of Health Sciences, Taizhou, Jiangsu, China.

Received: 15 May 2024 Accepted: 12 September 2024
Published online: 02 October 2024

References

1. Deary IJ, Corley J, Gow AJ, Harris SE, Houlihan LM, Marioni RE, et al. Age-associated cognitive decline. Brit Med Bull. 2009;92:135–52.
2. Wilson RS, Scherr PA, Schneider JA, Tang Y, Bennett DA. Relation of cognitive activity to risk of developing alzheimer disease. Neurology. 2007;69(20):1911–20.
3. Consortium AB, Jia Y-J, Wang J, Ren J-R, Chan P, Chen S, et al. A framework of biomarkers for brain aging: a consensus statement by the aging biomarker consortium. Life Med. 2023;2(3):lnad017.
4. Zecca L, Youdim MBH, Riederer P, Connor JR, Crichton RR. Iron, brain ageing and neurodegenerative disorders. Nat Rev Neurosci. 2004;5(11):863–73.
5. Ward RJ, Zucca FA, Duyn JH, Crichton RR, Zecca L. The role of iron in brain ageing and neurodegenerative disorders. Lancet Neurol. 2014;13(10):1045–60.
6. Lee J-H, Han Y-H, Kang B-M, Mun C-W, Lee S-J, Baik S-K. Quantitative assessment of subcortical atrophy and iron content in progressive supranuclear palsy and parkinsonian variant of multiple system atrophy. J Neurol. 2013;260(8):2094–101.
7. Damulina A, Pirpamer L, Soellradl M, Sackl M, Tinauer C, Hofer E, et al. Cross-sectional and longitudinal assessment of brain iron level in alzheimer disease using 3-T MRI. Radiology. 2020;296(3):619–26.
8. Langkammer C, Schweser F, Krebs N, Deistung A, Goessler W, Scheurer E, et al. Quantitative susceptibility mapping (QSM) as a means to measure brain iron? A post mortem validation study. NeuroImage. 2012;62(3):1593–9.
9. Harada T, Kudo K, Fujima N, Yoshikawa M, Ikebe Y, Sato R, et al. Quantitative susceptibility mapping: basic methods and clinical applications. Radiographics. 2022;42(4):1161–76.
10. Lane DJR, Ayton S, Bush AI. Iron and alzheimer's disease: An update on emerging mechanisms. Perry G, Avila J, Moreira PI, Sorensen AA, Tabaton M, editors. J Alzheimers Dis. 2018;64(s1):S379–95.
11. Ayton S, Fazlollahi A, Bourgeat P, Raniga P, Ng A, Lim YY, et al. Cerebral quantitative susceptibility mapping predicts amyloid-β-related cognitive decline. Brain. 2017;140(8):2112–9.
12. Spotorno N, Acosta-Cabronero J, Stomrud E, Lampinen B, Strandberg OT, van Westen D, et al. Relationship between cortical iron and tau aggregation in alzheimer's disease. Brain. 2020;143(5):1341–9.
13. Jiang Y, Cui M, Tian W, Zhu S, Chen J, Suo C, et al. Lifestyle, multi-omics features, and preclinical dementia among Chinese: the taizhou imaging study. Alzheimers Dement. 2021;17(1):18–28.
14. Shi L, Zhao L, Yeung FK, Wong SY, Chan RKT, Tse MF, et al. Mapping the contribution and strategic distribution patterns of neuroimaging features of small vessel disease in poststroke cognitive impairment. J Neurol Neurosur Ps. 2018;89(9):918–26.
15. Li H, Jia J, Yang Z. Mini-mental state examination in elderly Chinese: a population-based normative study. J Alzheimers Dis. 2016;53(2):487–96.
16. Lu J, Li D, Li F, Zhou A, Wang F, Zuo X, et al. Montreal cognitive assessment in detecting cognitive impairment in Chinese elderly individuals: a population-based study. J Geriatr Psych Neur. 2011;24(4):184–90.
17. American Psychiatric Association, editor. Diagnostic and statistical manual of mental disorders: DSM-5. 5th ed. Washington, D.C: American Psychiatric Association; 2013.
18. Petersen RC. Early diagnosis of alzheimer's disease: is MCI too late? Curr Alzheimer Res. 2009;6(4):324–30.
19. Hibar DP, Stein JL, Renteria ME, Arias-Vasquez A, Desrivières S, Jahanshad N, et al. Common genetic variants influence human subcortical brain structures. Nature. 2015;520(7546):224.
20. Chan K-S, Marques JP. SEPIA—susceptibility mapping pipeline tool for phase images. NeuroImage. 2021;227:117611.
21. Li W, Wu B, Liu C. Quantitative susceptibility mapping of human brain reflects spatial variation in tissue composition. NeuroImage. 2011;55(4):1645–56.
22. Wu B, Li W, Guidon A, Liu C. Whole brain susceptibility mapping using compressed sensing. Magn Reson Med. 2012;67(1):137–47.
23. Langkammer C, Bredies K, Poser BA, Barth M, Reishofer G, Fan AP, et al. Fast quantitative susceptibility mapping using 3D EPI and total generalized variation. NeuroImage. 2015;111:622–30.
24. Li W, Wu B, Batrachenko A, Bancroft-Wu V, Morey RA, Shashi V, et al. Differential developmental trajectories of magnetic susceptibility in human brain gray and white matter over the lifespan. Hum Brain Mapp. 2014;35(6):2698–713.
25. Betts MJ, Acosta-Cabronero J, Cardenas-Blanco A, Nestor PJ, Düzel E. High-resolution characterisation of the aging brain using simultaneous quantitative susceptibility mapping (QSM) and r2* measurements at 7T. NeuroImage. 2016;138:43–63.
26. Jack CR, Wiste HJ, Weigand SD, Knopman DS, Mielke MM, Vemuri P, et al. Different definitions of neurodegeneration produce similar amyloid/neurodegeneration biomarker group findings. Brain. 2015;138(Pt 12):3747–59.
27. Bakkour A, Morris JC, Wolk DA, Dickerson BC. The effects of aging and alzheimer's disease on cerebral cortical anatomy: specificity and differential relationships with cognition. NeuroImage. 2013;76:332–44.
28. Lee JE, Chung MK, Lazar M, DuBray MB, Kim J, Bigler ED, et al. A study of diffusion tensor imaging by tissue-specific, smoothing-compensated voxel-based analysis. NeuroImage. 2009;44(3):870–83.
29. Benjamini Y, Hochberg Y. Controlling the false discovery rate: a practical and powerful approach to multiple testing. J R Stat Soc Ser B Stat Methodol. 1995;57(1):289–300.
30. Zachariou V, Bauer CE, Seago ER, Raslau FD, Powell DK, Gold BT. Cortical iron disrupts functional connectivity networks supporting working memory performance in older adults. NeuroImage. 2020;223:117309.
31. Ravanfar P, Loi SM, Syeda WT, Van Rheenen TE, Bush AI, Desmond P, et al. Systematic review: quantitative susceptibility mapping (QSM) of brain iron profile in neurodegenerative diseases. Front Neurosci. 2021;15:618435.
32. Howard CM, Jain S, Cook AD, Packard LE, Mullin HA, Chen N, et al. Cortical iron mediates age-related decline in fluid cognition. Hum Brain Mapp. 2022;43(3):1047–60.
33. Dixon SJ, Stockwell BR. The role of iron and reactive oxygen species in cell death. Nat Chem Biol. 2014;10(1):9–17.
34. Urrutia PJ, Bórquez DA, Núñez MT. Inflaming the brain with iron. Antioxid (Basel). 2021;10(1):61.
35. Jia X, Wang Z, Huang F, Su C, Du W, Jiang H, et al. A comparison of the Mini-mental State Examination (MMSE) with the Montreal Cognitive Assessment (MoCA) for mild cognitive impairment screening in Chinese middle-aged and older population: a cross-sectional study. BMC Psychiatry. 2021;21(1):485.
36. Jobson DD, Hase Y, Clarkson AN, Kalaria RN. The role of the medial prefrontal cortex in cognition, ageing and dementia. Brain Commun. 2021;3(3):fcab125.
37. Dixon SJ, Lemberg KM, Lamprecht MR, Skouta R, Zaitsev EM, Gleason CE, et al. Ferroptosis: an iron-dependent form of nonapoptotic cell death. Cell. 2012;149(5):1060–72.
38. Xia C, Makaretz SJ, Caso C, McGinnis S, Gomperts SN, Sepulcre J, et al. Association of in vivo [18F]AV-1451 tau PET imaging results with cortical atrophy and symptoms in typical and atypical alzheimer disease. JAMA Neurol. 2017;74(4):427–36.
39. Ndayisaba A, Kaindlstorfer C, Wenning GK. Iron in neurodegeneration - cause or consequence? Front Neurosci. 2019;13:180.
40. Daugherty AM, Raz N. Accumulation of iron in the putamen predicts its shrinkage in healthy older adults: a multi-occasion longitudinal study. NeuroImage. 2016;128:11–20.
41. Kan H, Uchida Y, Arai N, Ueki Y, Aoki T, Kasai H, et al. Simultaneous voxel-based magnetic susceptibility and morphometry analysis using magnetization-prepared spoiled turbo multiple gradient echo. NMR Biomed. 2020;33(5):e4272.
42. Yang A, Du L, Gao W, Liu B, Chen Y, Wang Y, et al. Associations of cortical iron accumulation with cognition and cerebral atrophy in alzheimer's disease. Quant Imag Med Surg. 2022;12(9):4570–86.
43. Sun Y, Ge X, Han X, Cao W, Wang Y, Ding W, et al. Characterizing brain iron deposition in patients with subcortical vascular mild cognitive impairment using quantitative susceptibility mapping: a potential biomarker. Front Aging Neurosci. 2017;9:81.
44. Gregory A, Hayflick SJ. Genetics of neurodegeneration with brain iron accumulation. Curr Neurol Neurosci. 2011;11(3):254–61.

45. Chen L, Soldan A, Oishi K, Faria A, Zhu Y, Albert M, et al. Quantitative susceptibility mapping of brain iron and β-amyloid in MRI and PET in cognitively normal older adults. Radiology. 2021;298(2):353–62.
46. Acosta-Cabronero J, Betts MJ, Cardenas-Blanco A, Yang S, Nestor PJ. In vivo MRI mapping of brain iron deposition across the adult lifespan. J Neurosci. 2016;36(2):364–74.
47. Burgetova R, Dusek P, Burgetova A, Pudlac A, Vaneckova M, Horakova D, et al. Age-related magnetic susceptibility changes in deep grey matter and cerebral cortex of normal young and middle-aged adults depicted by whole brain analysis. Quant Imag Med Surg. 2021;11(9):3906–19.
48. Olmedo-Díaz S, Estévez-Silva H, Orädd G, Af Bjerkén S, Marcellino D, Virel A. An altered blood-brain barrier contributes to brain iron accumulation and neuroinflammation in the 6-OHDA rat model of parkinson's disease. Neuroscience. 2017;362:141–51.
49. Devos D, Labreuche J, Rascol O, Corvol J-C, Duhamel A, Guyon Delannoy P, et al. Trial of deferiprone in parkinson's disease. N Engl J Med. 2022;387(22):2045–55.
50. Krebs N, Langkammer C, Goessler W, Ropele S, Fazekas F, Yen K, et al. Assessment of trace elements in human brain using inductively coupled plasma mass spectrometry. J Trace Elem Med Biol. 2014;28(1):1–7.
51. Fukunaga M, Li T-Q, Van Gelderen P, De Zwart JA, Shmueli K, Yao B, et al. Layer-specific variation of iron content in cerebral cortex as a source of MRI contrast. Proc Natl Acad Sci U S A. 2010;107(8):3834–9.
52. Zhao Y, Wen J, Cross AH, Yablonskiy DA. On the relationship between cellular and hemodynamic properties of the human brain cortex throughout adult lifespan. NeuroImage. 2016;133:417–29.

Publisher's note